



## Fe<sub>2</sub>O<sub>3</sub> thin films prepared by spray pyrolysis technique and study the annealing on its urbach energy and dispersion parameters

Khalid Haneen Abass

Department of Physics, College of Education for Pure Sciences, University of Babylon, (IRAQ)

### ABSTRACT

In this paper, we study the Urbach energy and dispersion parameters of Fe<sub>2</sub>O<sub>3</sub> thin films that doped by 1% NiO prepared by Chemical pyrolysis method. The prepared films are annealed at 450 °C and 500 °C and then it recorded the optical absorption spectra by UV-Visible spectrophotometer in the range of (300-900) nm. The absorbance and Urbach energy increase with increasing annealing temperature for NiO:Fe<sub>2</sub>O<sub>3</sub> thin films, while  $\epsilon_1$  and  $\epsilon_2$  decrease with increasing annealing temperature. The Wemple and Didomenico dispersion relationship that used to determine dispersion parameters. Energy gap calculated from  $E_m = 2E_g$ , which found it decreases with annealing temperature from 2.68 eV before annealed to 2.57 eV after 500 °C. Dispersion parameters such as  $E_d$ ,  $E_m$ ,  $\epsilon_\infty$ ,  $n(0)$ ,  $M_{-1}$ , and  $M_{-3}$  are decreased with annealing temperatures. © 2015 Trade Science Inc. - INDIA

### KEYWORDS

Fe<sub>2</sub>O<sub>3</sub> thin film;  
Annealing, urbach energy;  
Dispersion parameters.

### INTRODUCTION

Iron oxide (Fe<sub>2</sub>O<sub>3</sub>) in hematite crystalline structure has recently attracted much attention as a possible convenient material to be used for hydrogen production via photoelectrochemical (PEC) water splitting. It is due to its favorable properties such as a band gap between 2.0 - 2.2 eV, which allows absorbing a substantial fraction of solar spectrum, chemical stability in aqueous environment, nontoxicity, abundance, and low cost. For such band gap and assuming the standard solar illumination conditions (AM 1.5 G, 100 mW cm<sup>-2</sup>) theoretical maximal solar-to-hydrogen (STH) conversion efficiency can be calculated as 15 %<sup>[1]</sup>. Earlier investigations have shown that the Fe<sub>2</sub>O<sub>3</sub> is a promising semiconductor anode for the photo- decomposition

of water in a PEC cell<sup>[2]</sup>. The Fe<sub>2</sub>O<sub>3</sub> is a robust room-temperature insulating ferrimagnet with a Curie temperature of about 500 K<sup>[3]</sup>, which is driving current interest for possible applications<sup>[4]</sup>.

On account of these favorable characteristics, many authors have studied the potential of using hematite in solar energy conversion prepared by different routes, e.g. pressing of material into pellets<sup>[5-7]</sup>, sputtering<sup>[8-9]</sup>, spray pyrolysis<sup>[10-11]</sup>, pulsed laser deposition (PLD)<sup>[12]</sup>, and molecular beam epitaxy<sup>[13]</sup>.

Nanostructured and nanorods of hematite have also been studied for PECsplitting of water<sup>[14-15]</sup>.

Present work is to study the effect of annealing temperature (before annealing, 400°C and 500 °C) on Urbach energy and dispersion parameters of NiO:Fe<sub>2</sub>O<sub>3</sub> thin films that prepared by chemical spray pyrolysis method.

## Full Paper

### EXPERIMENTAL

Thin films of Nickel oxide doped Fe<sub>2</sub>O<sub>3</sub> have been prepared by chemical pyrolysis technique. A laboratory designed glass atomizer was used for spraying the aqueous solution, which has an output nozzle about 1 mm. The films were deposited on preheated cleaned glass substrates at a temperature of 400 °C. A 0.1 M for both NiCl<sub>2</sub> (Sigma Aldrich UK) and FeCl<sub>3</sub> (Merck Chemicals Germany) diluted with redistilled water and a few drops of HCl were used to obtain the starting solution for deposition. Moreover, volumetric concentration of NiO 1% was achieved the optimized conditions have been arriving at the following parameters; spray time was 10 s and the spray interval 2 min was kept constant. The carrier gas (filtered compressed air) was maintained at a pressure of 10<sup>5</sup> Nm<sup>-2</sup>, and the distance between nozzle and substrate was about 30 cm ± 1 cm.

Thickness of the sample was measured using the weighting method and was found to be around 400 nm. Optical transmittance and absorbance were recorded in the wavelength range of (300-900) nm using UV-Visible spectrophotometer (Shimadzu Company Japan).

### RESULTS AND DISCUSSIONS

The optical absorbance of the NiO:Fe<sub>2</sub>O<sub>3</sub> thin films are represented in Figure 1. It can be seen that

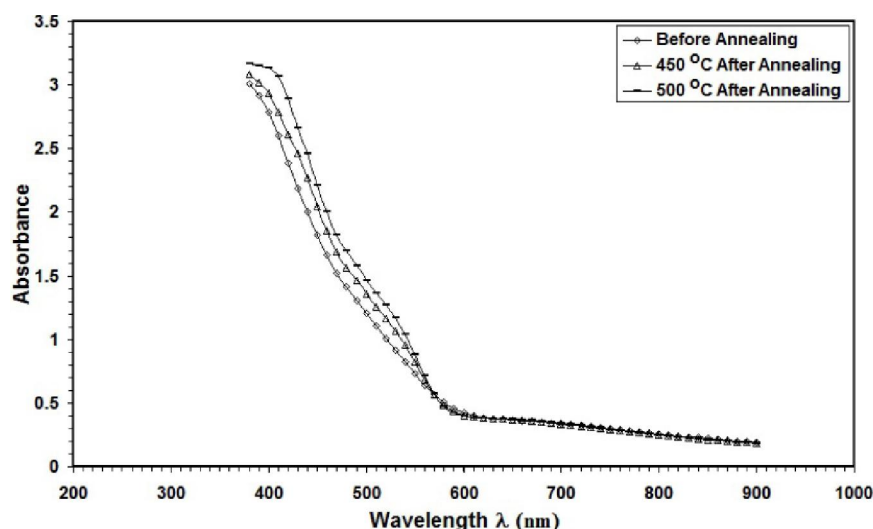


Figure 1 : Plot of absorbance as a function of the wavelength for the NiO-doped Fe<sub>2</sub>O<sub>3</sub> thin films with different annealing temperatures

the absorbance takes the same values in the NIR region ( $\lambda > 580$  nm), only from about 580 nm wavelength it can observe a difference on the absorption spectra of the prepared films. In addition, it can be seen that the absorbance increases with increasing annealing temperature.

The real ( $\epsilon_1$ ) and imaginary ( $\epsilon_2$ ) parts of the dielectric constant ( $\epsilon = \epsilon_1 + i\epsilon_2$ ) may be related to the real part of refractive index ( $n$ ) and the extinction coefficient ( $K$ )<sup>[16]</sup>:

$$\epsilon_1 = n^2 - K^2 \quad (1)$$

$$\epsilon_2 = 2nK \quad (2)$$

Figure 1 and Figure 2 represent the relationship between real and imaginary parts of dielectric constants with wavelength. It's clear from these figures that the  $\epsilon_1$  and  $\epsilon_2$  decreases with increasing annealing temperature until the wavelength of 580 nm, and then the annealing temperature don't changes the dielectric constants.

The optical conductivity ( $\sigma$ ) was calculated using the relation<sup>[17]</sup>:

$$\sigma = \frac{\alpha n c}{4\pi} \quad (3)$$

Where  $\alpha$  is the absorption coefficient,  $n$  is the refractive index, and  $c$  represent the velocity of light. Optical conductivity versus wavelength is shown in Figure 4. From this figure, it can notice that the optical conductivity decreases with increasing annealing temperature until the wavelength of 470 nm, and

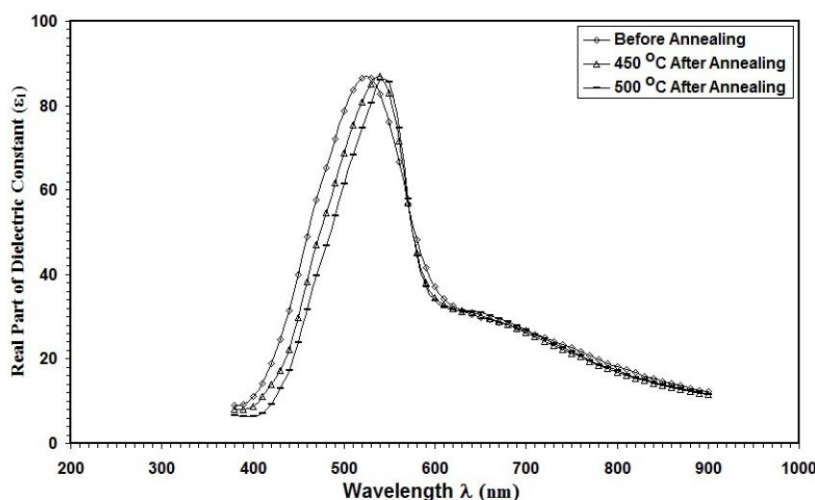


Figure 2 : Plot of real part of dielectric constant as a function of the wavelength for the NiO-doped  $\text{Fe}_2\text{O}_3$  thin films with different annealing temperatures

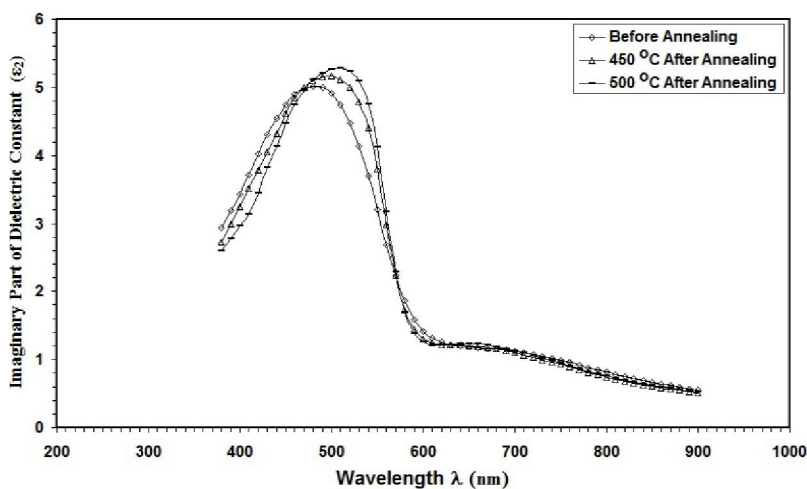


Figure 3 : Plot of imaginary part of dielectric constant as a function of the wavelength for the NiO-doped  $\text{Fe}_2\text{O}_3$  thin films with different annealing temperatures

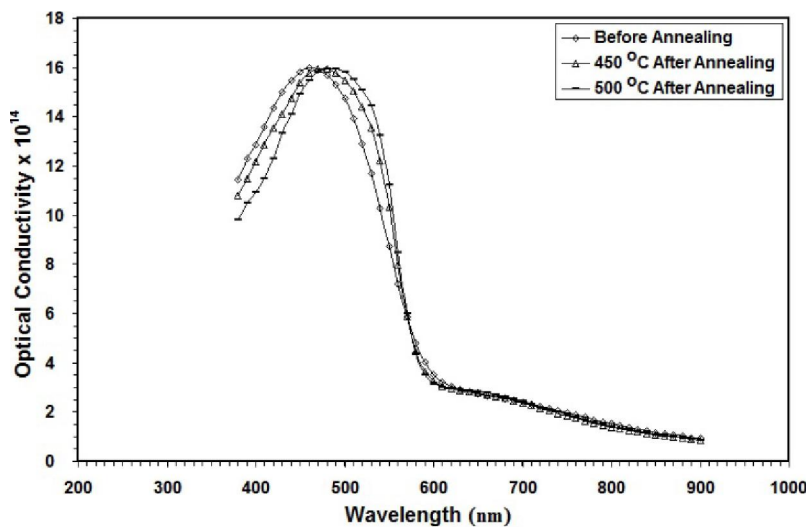


Figure 4 : Plot of optical conductivity as a function of the wavelength for the NiO-doped  $\text{Fe}_2\text{O}_3$  thin films with different annealing temperatures

## Full Paper

then increases with increasing annealing temperature until 580 nm. After this the optical conductivity still stable with wavelength at various temperatures.

The Urbach tail of the films can be determined by the following relation<sup>[18]</sup>:

$$\alpha = \alpha_0 \exp\left[\frac{E}{E_U}\right] \quad (4)$$

Where E is the photon energy (hν), α<sub>0</sub> is constant, and E<sub>U</sub> is the Urbach energy that refers to the width of the exponential absorption edge. Figure 5 shows the variation of lnα vs. hν for the NiO:Fe<sub>2</sub>O<sub>3</sub> thin films. This behavior corresponds primarily to optical transitions between occupied states in the valence band tail to unoccupied states at the conduction band edge. Urbach energy values of the films increase with increasing NiO content as listed in

TABLE 1. The E<sub>U</sub> values change inversely with optical band gaps of the films.

A single-oscillator model was also used to fit the energy dependence of refractive index, namely, the Wemple and Didomenico dispersion relationship<sup>[19]</sup>:

$$n^2(E) = 1 + \frac{E_m E_d}{E_m^2 - E^2} \quad (5)$$

Where E<sub>m</sub> and E<sub>d</sub> is the single-oscillator and dispersion energy, respectively, and E is the photon energy (hν). (n<sup>2</sup>-1)<sup>-1</sup> vs. E<sup>2</sup> is plotted in Figure 6. It indicates that the refractive index correspond the model as a straight line fitted to the data.

A plot of (n<sup>2</sup>-1)<sup>-1</sup> versus 1/λ<sup>2</sup> (see Figure 7) would be linear with a negative slope and give the values of E<sub>0</sub> and E<sub>d</sub> from the slope (1/E<sub>m</sub>E<sub>d</sub>) and the inter-

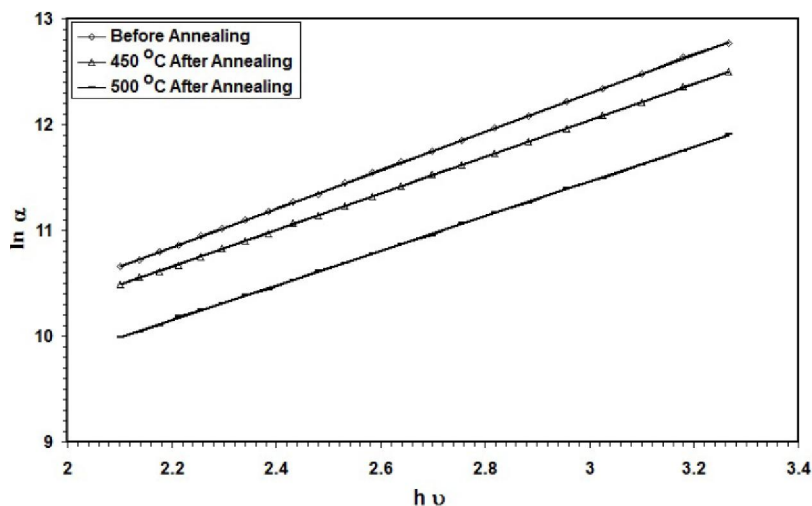


Figure 5 : Ln(α) versus hν for the NiO-doped Fe<sub>2</sub>O<sub>3</sub> thin films with different annealing temperatures

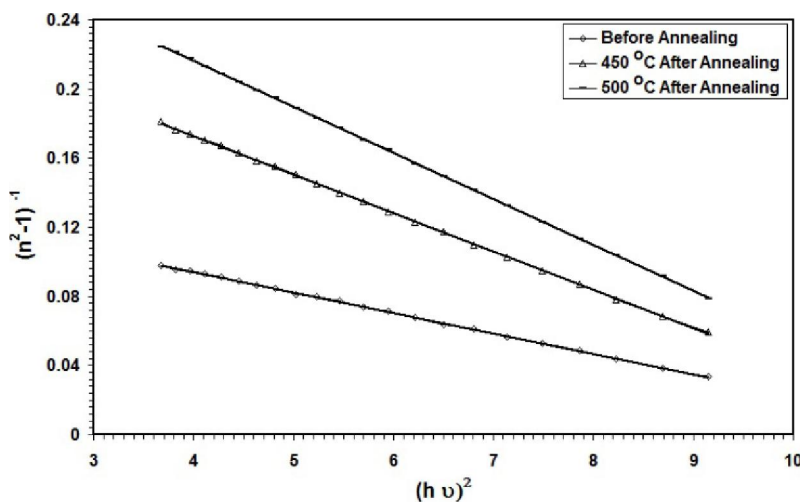


Figure 6 : (n<sup>2</sup>-1)<sup>-1</sup> versus (hν)<sup>2</sup> for the NiO-doped Fe<sub>2</sub>O<sub>3</sub> thin films with different annealing temperatures

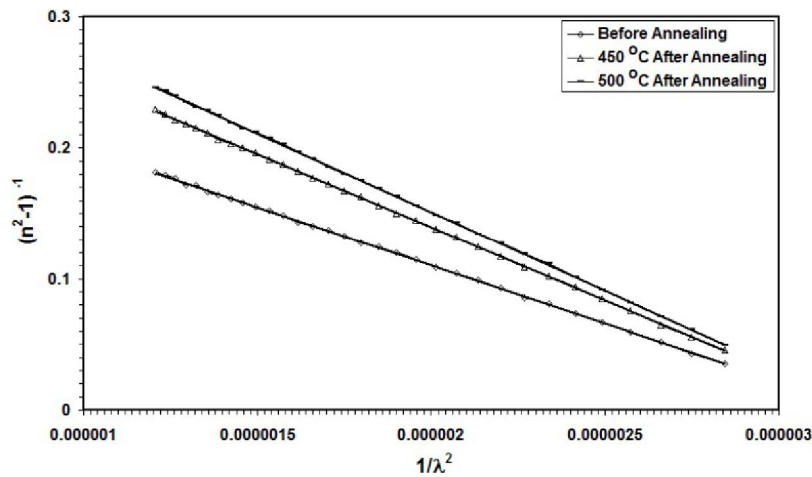


Figure 7 :  $(n^2-1)^{-1}$  versus  $(1/\lambda^2)$  for the NiO-doped  $\text{Fe}_2\text{O}_3$  thin films with different annealing temperatures

TABLE 1 : The optical parameters of NiO: $\text{Fe}_2\text{O}_3$  thin films

Sample	$E_d$ (eV)	$E_o$ (eV)	$E_g$ (eV)	$\epsilon_\infty$	$n(o)$	$M_{-1}$	$M_{-3}$ ( $\text{eV}^{-2}$ )	$S_o \times 10^{13}$ ( $\text{m}^{-2}$ )	$\lambda_o$ (nm)	$E_U$ (meV)
Before Annealing	48.70	5.36	2.68	10.26	3.17	9.10	0.315	3.35	385	555
450 °C After Annealing	27.60	5.24	2.62	6.26	2.50	5.26	0.191	2.69	392	574
500 °C After Annealing	22.35	5.14	2.57	5.34	2.31	4.34	0.164	2.53	397	606

cept on the y-axis ( $E_m/E_d$ ). The parameter  $E_m$  is an average energy gap and can be related by an empirical formula to the optical band gap value:  $E_m = 2E_g$  [20].

The refractive index  $n(0)$  at zero photon energy, which is defined by the infinite wavelength dielectric constant, can be deduced from the dispersion relationship by extrapolation of the linear part.

The refractive index has been analyzed to yield the high frequency dielectric constant ( $\epsilon_\infty = n_\infty^2$ ) [21-22]. Assuming the high-frequency properties could be treated as a single oscillator at wavelength  $\lambda_o$  at high frequency. The high-frequency dielectric constant can be calculated by the following classical dispersion relation [22]:

$$\frac{n_\infty^2 - 1}{n^2 - 1} = 1 - \left( \frac{\lambda_o}{\lambda} \right)^2 \quad (6)$$

Where  $n_\infty$  is the refractive index at infinite wavelength ( $\lambda_o$ ) (average oscillator wavelength),  $n$  is the refractive index and  $\lambda$  is the wavelength of the incident photon. The plots of  $(n^2-1)^{-1}$  vs.  $\lambda^{-2}$  were plotted to obtain  $n_\infty$  values and listed in TABLE 1.

The  $M_{-1}$  and  $M_{-3}$  moments of the optical spectra can be obtained from the following relations [23]:

$$E_o^2 = \frac{M_{-1}}{M_{-3}} \quad (7)$$

$$E_d^2 = \frac{M_{-1}^3}{M_{-3}} \quad (8)$$

The obtained  $M_{-1}$  and  $M_{-3}$  moments changes with the annealing temperature as listed in TABLE 1.

## CONCLUSION

The  $\text{Fe}_2\text{O}_3$  thin films that doped of 0.1% NiO prepared by chemical spray pyrolysis method, and annealed at 450 and 500 °C respectively. The absorbance spectra were recorded in the range of 300-900 nm, and then calculated the dispersion parameters from Wemple and Didomenico dispersion relationship. Dispersion parameters such as  $E_d$ ,  $E_m$ ,  $\epsilon_\infty$ ,  $n(0)$ ,  $M_{-1}$ , and  $M_{-3}$  are decreased with annealing temperatures, while the Urbach energy increased with increasing annealing temperature for all NiO: $\text{Fe}_2\text{O}_3$  thin films that inversely proportion with energy gap which decreased from 2.68 to 2.57 eV.

## REFERENCES

- [1] K.Sivula, F.Le Formal, M.Grätzel; Solar water splitting: Progress using hematite ( $\alpha\text{-Fe}_2\text{O}_3$ ) Photoelectrodes, Chem.Sus.Chem, **4**, 432 (2011).
- [2] M.P.Darewards, J.B.Goodenough, A.Hamnett,

**Full Paper**

- P.R.Trevellick; J.Chem.Sot.FaradayTrans.I., **79**, 2027 (1983).
- [3] R.Schrader, G.Buttner, Z.Anorg; Allg.Chem., **320**, 220 (1963).
- [4] A.Namai, S.Sakurai, M.Nakajima, T.Suemoto, K.Matsumoto, M.Goto, S.Sasaki, S.i.Ohkoshi; J.Am.Chem.Soc., **131**, 1170 (2009); b) B.Jin, S.Ohkoshi, K.Hashimoto; Adv.Mater., **16**, 48 (2004).
- [5] C.Leygraf, M.Hendewerk, G.A.Somorjai; Mg-and Si-doped iron oxides for the photocatalyzed production of hydrogen from water by visible light ( $2.2 \text{ eV} < h\nu < 2.7 \text{ eV}$ ), J.Catal., **78**, 341 (1982).
- [6] K.Gurunathan, P.Maruthamuthu; Photogeneration of hydrogen using visible light with undoped/doped  $\alpha\text{-Fe}_2\text{O}_3$  in the presence of methyl viologen, Int.J.Hydrogen Energy, **20**, 287 (1995).
- [7] V.M.Aroutiounian, V.M.Arakelyan, G.E.Shahnazaryan, G.M.Stepanyan, J.A.Turner, O.Khaselev; Investigation of ceramic ( $\text{Fe}_2\text{O}_3$ )(Ta) photoelectrodes for solar energy photoelectrochemical converters, Int.J.Hydrogen Energy, **27**, 33 (2002).
- [8] S.Virtanen, P.Schmuki, H.Böhni, P.T.Vuoristo; Artificial Cr-and Fe-oxide passive layers prepared by sputter deposition, J.Electrochem.Soc., **142**, 3067 (1995).
- [9] J.P.Hong, S.B.Lee, Y.W.Jung, J.H.Lee, K.S.Yoon, K.W.Kim, C.H.Lee, M.H. Jung; Appl.Phys.Lett., **83**, 1590 (2003).
- [10] S.U.M.Khan, J.Akikusa; Photoelectrochemical splitting of water at nanocrystalline- $\text{Fe}_2\text{O}_3$  thin-film electrodes, J.Phys.Chem.B, **103**, 7184 (1999).
- [11] T.Lindgren, L.Vayssieres, H.Wang, S.E.Lindquist; Chemical physics of nanostructured semiconductors (eds Kokorin, A.I. and Bahnemann, D.W.), VSP, Utrecht, The Netherlands, 93 (2003).
- [12] T.Tepper, C.A.Ross; J.Appl.Phys., **91**, 4453 (2002).
- [13] T.Hibma, F.C.Voogt, L.Niesen, P.A.A.Van Der Heijden, W.J.M.De Jonge, J.J.T.M.Donkers, P.J.Van Der Zaag; J.Appl.Phys., **85**, 5291 (1999).
- [14] U.Björkstén, J.Moser, M.Grätzel; Photoelectrochemical studies on nanocrystalline hematite films, Chem.Mater., **6**, 858 (1994).
- [15] L.Vayssieres, N.Beer mann, S.E.Lindquist, A.Hagfeldt; Controlled aqueous chemical growth of oriented three-dimensional nanorod arrays: application to iron(III) oxides, Chem.Mater., **13**, 233 (2001).
- [16] J.N.Hodgson; "Optical absorption and dispersion in solids", Chapman and Hall Ltd., 11 New Fetter Lane.London EC4, (1970).
- [17] J.I.Pankove; "Optical processes in semiconductors", Dover Publications, Inc.New York, 91 (1975).
- [18] F.Urbach; Phys.Rev., **92**, 1324 (1953).
- [19] S.H.Wemple, M.DiDomenico; Phys.Rev., B, **3**, 1338–1350 (1971).
- [20] M.Modreanu, M.Gartner, N.Tomozeiu, J.Seekamp, P.Cosmin; Opt.Mater., **17**, 145 (2001).
- [21] J.N.Zemel, J.D.Jensen, R.B.Schoolar; Phys.Rev.A, **140**, 330 (1965).
- [22] T.S.Moss; Optical properties of semiconductors, Butter WortsScientific publication Ltd., London, (1959).
- [23] M.Modreanu, M.Gartner, N.Tomozeiu, J.Seekamp, P.Cosmin; Opt.Mater., **17**, 145 (2001).